JOURNAL OF PROPULSION AND POWER
Vol. 14, No. 4, July–August 1998

Strategies for Pulsed Detonation Engine Performance Optimization

J.-L. Cambier*
FFA, Aeronautical Research Institute of Sweden, Bromma S-161 11, Sweden
and
J. K. Tegnér†
FOA, Stockholm S-172 90, Sweden

The pulsed detonation engine (PDE) concept is systematically analyzed with respect to design variations, and the potential performance is measured from computational fluid dynamics simulations. Variations in configuration geometry are examined first through single-pulse computations. These show that the presence of a nozzle can greatly affect the performance of the PDE by increasing thrust delivery during the ignition phase. It is further shown that it is not necessary to fill the entire tube with a fuel–air mixture and that significant gains in specific impulse can be obtained by appropriate fueling strategies. Multicycle computations are performed next and the effect of cycling parameters is studied. It is shown that the cycling frequency can be significantly increased by selecting the pressure parameters and the extent of refueling. We also show that multicycle performance can be very different from the single-pulse estimates, and that it is not possible to optimize separately the ignition phase from the injection phase. Finally, the question of open-end initiation is examined and a comparison between quasi-one-dimensional and two-dimensional computations is performed.

Nomenclature

F = force (thrust)
$\dot{m}$ = mass flow
P = pressure
S = surface
$\boldsymbol{u}$ = velocity
V = volume
α, β = inverse time scales (pulse shape)
η = inverse length scale (nozzle shape)
η_u = relative thrust efficiency
ρ = mass density

Subscripts
$a(P_a)$ = ambient (external pressure)
$c(P_c)$ = chamber (critical chamber pressure)
$r(P_r)$ = reservoir (fuel reservoir pressure)
w, e, i = walls, exit plane, inlet plane, respectively

I. Introduction

PULSED detonation engines (PDE) are currently the focus of increasing interest and the subject of several analytical and experimental investigations.[1] PDEs belong to a general class of unsteady flow devices with high-performance potential.[2] However, their analysis is made difficult by the nonsteady dynamics, and the design rules previously applied to steady flow conditions may not be applicable for this new class of engines. For example, one important difference between unsteady and steady engines concerns the matching of ambient conditions. The rocket nozzle performance is optimized when the pressure at the exit plane is the same as the ambient pressure, but this simple criterion is not applicable in the unsteady case because the pressure field at the exit plane is not steady, thus making the problem of nozzle optimization more difficult. This is where performance losses may occur. At the end of the blowdown phase of the cycle, both static and dynamic pressures at the exit are low. There may be a time within the cycle where the thrust is dominated by the first term in the right-hand side (RHS) of Eq. (4), and be negative, i.e., $p_e < p_a$. One of the challenges in PDE design is also to minimize the losses during this part of the cycle.

The operation of the unsteady engine must also be optimized with respect to the cycling frequency. Clearly, it is not only desirable to produce high peak and average values of the pressure but also to repeat the cycles as fast as possible. The cycling will be faster if the tube is short and if rapid expansion takes place at the tube exit. A nozzle may affect the time required for the pressure in the tube to drop to a specific value, at which time a fresh mixture can be injected. It is therefore necessary to systematically investigate the effects of a nozzle on a PDE performance, as well as various fueling and ignition strategies. This paper presents a preliminary work in that direction by analyzing single pulses as well as multicycle operation.

In all previous calculations of PDE performance[3–13] there has been a number of assumptions made to simplify the task, and most of these assumptions are being repeated here. For example, a common simplification is the suppression of the chemical reactions during the injection phase. This is done to avoid immediate burning of the fresh mixture as it comes in contact with the hot products from the previous cycle. This premature ignition can be alleviated by the introduction of a buffer gas, and by ignoring this buffering we allow for faster cycling and higher performance. Eventually, one must deal with the evaluation of the required thickness of the buffer, its efficiency, and the associated cycling penalties. This will require multidimensional Navier–Stokes calculations (the interfaces would be subject to Rayleigh–Taylor instabilities), and would depend on the exact injector location and geometry. One should also investigate its effectiveness at preventing ignition from hot spots on the chamber walls.

Presented as Paper 97-2743 at the AIAA/ASME/SAE/ASEE 33rd Joint Propulsion Conference, Seattle, WA, July 6–9, 1997; received Oct. 9, 1997; revision received Feb. 6, 1998; accepted for publication Feb. 8, 1998.

*Computational Fluid Dynamics Department; currently Staff Scientist, MSE-TA, Inc., P.O. Box 4078, Butte, MT 59701. Member AIAA.

†Research Engineer, Warheads and Propulsion Department.

Instantaneous valve action is another common assumption; real valves open and close within a finite time, and this should also be considered as a penalty in cycling frequency. The mixing between fuel and oxidizer is another issue that has not yet been examined in detail. Its correct evaluation is difficult and depends strongly on the injector geometries, turbulence levels, and multidimensional effects. By injecting premixed gases in the chamber, the problem is simplified, and the cycling frequency of this ideal case is increased compared with a real engine.

Finally, another important simplification consists of modeling the detonation initiation by having a sufficiently large energy deposition. This is one of the most fundamental difficulties in PDE operation. Means of providing this initiation energy must be devised and they are an important factor in estimating the overall engine performance. If on the other hand one relies on the natural deflagration to detonation transition (DDT), the energy requirement is much lower, but the process itself presents problems; notably, it is not exactly reproducible and it requires additional time (another cycling penalty) and distance (a possible weight penalty). Although there has been recent progress toward a full understanding of DDT,[14] accurate and predictive modeling of the process is a very difficult task. Although most of these neglected processes can be computed and included in the analysis, it is an expensive proposition, and for limited computing resources, the best strategy would be to include them once the more elementary processes are completely understood. It is clear that with all these approximations we can only achieve an ideal operating regime and reasonably estimate its performance accuracy. Therefore, numerical optimization is best used to provide a theoretical upper limit to the PDE performance and insights into the best designs and engine configurations.

There are also several levels of complexity for which the performance of a PDE can be investigated. Some studies are done for a single-cycle only PDE,[5–8,12,13] and others are done in quasi-one-dimensional PDE.[3,8–10] The calculations can also be performed for static conditions[3] or flight conditions. In the latter case, optimization with respect to ambient conditions and inlet design adds to the complexity. In Ref. 5, a number of test cases were computed, and it was concluded that the performance was strongly dependent on the inlet area and suffered from high wave drag at high Mach numbers. Pegg et al.[15] found it possible to design an inlet/isolator and plenum chambers for a realistic PDE engine configuration, such that inlet unstart is prevented. The isolator uses boundary-layer bleeding for shock stabilization, a technique also used in ramjet engine design. There seems to be two schools of thought on the ignitor location. Eidelman et al.[5–8] claimed that the best performance was obtained for open-end ignition, i.e., when the detonation wave travels upstream to impact on the thrust surface at the closed end of the tube; whereas the one-dimensional calculations performed in Ref. 9 showed an equivalent performance between closed- and open-end ignition.

There are some results that are of general interest and are without controversy. The most important of these is the performance scaling law with respect to chamber volume and cycle frequency, verified by Eidelman et al.[5] Computations have been performed for a number of configurations, fuels, and flight conditions. For this reason, the computed performance results can show some significant variations: Computed frequencies range from 200 to nearly 1 kHz, and the specific impulses from 3200 to 6500 s. Nevertheless, compared to the data for typical turbojets, it is believed that the PDE performance is encouraging from the point of view of thrust, thrust control, simplicity of the device, and specific fuel consumption. On the experimental side the situation is not quite as good, but this is only an indication of the difficulty associated with the manufacturing of the engine itself as well as on how far from reality the simulations still are. Early PDE experiments were able to demonstrate repeated detonations at 20 Hz.[16] Later experiments were able to cycle at 100 Hz, and this appears to be the current limit of the hardware designs.[17,18] There is no doubt, however, that the situation will improve in the near future. In the meantime, performance analysis can still provide important information on the nature of the optimizing parameters, until the time that calculations with more detailed physical models are performed.

Because the nonsteady dynamics complicate the performance analysis, it is quite necessary to perform systematic parametric studies, develop additional scaling laws, and develop a performance database for generic PDE configurations to obtain a better understanding of the engine characteristics for overall engine design and vehicle integration. This paper is a first attempt in this direction and also includes some analytical considerations.

II. Analytical Considerations

The PDE operation is based on periodic, unsteady flows and the performance analysis must be conducted appropriately. If one considers a simple control volume that contains the detonation tube, the evolution of the system is governed by the Euler (or Navier–Stokes) equations integrated over the entire control volume. An equation for the conservation of momentum can be written as

$$\int_V \left(\frac{\partial}{\partial t}\rho \boldsymbol{u}\right) \mathrm{d}V + \oint_S \mathrm{d}S(pI + \rho \boldsymbol{u} \otimes \boldsymbol{u}) = 0 \tag{1}$$

Here ρ, u, and p represent the density, velocity vector, and pressure (for the sake of simplicity source terms are not included). The integrations proceed over the entire control volume V and along its closed surface. If the system evolution is periodic in time and if one integrates over one period, the first term cancels out, because (for constant geometry)

$$\int_{\Delta t} \left(\frac{\partial}{\partial t}\rho \boldsymbol{u} V\right) \mathrm{d}t = V[(\rho \boldsymbol{u})_{t+\Delta t} - (\rho \boldsymbol{u})_t] \equiv 0 \tag{2}$$

Denoting the period-averaged quantities by brackets, we have a relation between the average pressure forces on the walls w and the average dynamic pressure at the exhaust e and inlet i boundaries:

$$\int_{S_w} \langle p_w \rangle \, \mathrm{d}S_w + \langle p_a \rangle \cdot S_i + \langle \rho_a u_a^2 \rangle \cdot S_i = \langle p_e \rangle \cdot S_e + \langle \rho_e u_e^2 \rangle \cdot S_e \tag{3}$$

Again, to simplify matters, it is assumed here that there is no velocity component normal to the solid walls. If there is, the dynamic pressure at the wall (ρu_n^2) should also be accounted for. We can now write the following expression for the average engine thrust, using the fact that the integral over all thrust wall surfaces is also related to the exit and inlet areas, $\int \mathrm{d}S_w \equiv S_e - S_i$:

$$\langle F \rangle = \int_{S_w} [\langle p_w \rangle - \langle p_a \rangle] \, \mathrm{d}S = \langle p_e - p_a \rangle \cdot S_e + \langle \rho_e u_e^2 \rangle \cdot S_e - \langle \rho_a u_a^2 \rangle \cdot S_i \tag{4}$$

Except for the averaging symbol, this relation is identical to the one obtained for steady flows. However, the instantaneous thrust will be different from the corresponding instantaneous quantities of the RHS of Eq. (4). This is quite obvious from the nature of the PDE operation itself. For example, if an explosion is initiated at the closed end of a tube, there is a force instantaneously applied to the structure, whereas the flow at the exit would be unaffected for some time, until the pressure waves reach the open end of the tube. Because we may also

need to look at interactions between several tubes, it is appropriate to keep track of the true instantaneous forces present in the engine. Using computational fluid dynamics (CFD) techniques, this can be easily done by integrating the pressure (and wall stresses if one computes Navier–Stokes solutions) along the entire surface of the engine. Both internal and external surfaces can be considered separately and all force components can be measured to evaluate the moments.

For the static case, i.e., zero ambient velocity, the last term on the RHS of Eq. (4) disappears. It is also interesting to point out that when a nozzle is added to the PDE, the exit pressure drops well below the dynamic pressure. In that case, the RHS of Eq. (4) is dominated by the $\langle \rho_e u_e^2 \rangle S_e$ term, which can also be written as $\langle \dot{m}_e u_e \rangle$, where $\dot{m}_e$ is the total, instantaneous mass flow in kg/s. If the performance of the PDE is compared with that of a steady rocket engine with the same average mass flow $\langle \dot{m}_e \rangle$ and the same average exit velocity $\langle u_e \rangle$, the thrust ratio is

$$\eta_u = \frac{\langle \dot{m}_e u_e \rangle}{\langle \dot{m}_e \rangle \langle u_e \rangle} \tag{5}$$

Notice that a performance gain is achieved by using an unsteady propulsion device for which there is a strong correlation between the mass flow and the velocity at the exit plane. Such is the case of strong blast waves. Without going through the exact expression of blast-wave profiles, let us assume that both density and velocity fields take an approximate exponential variation

$$\rho_e = \rho_1 e^{-\alpha t}, \qquad u_e = u_1 e^{-\beta t}$$

where ρ_1 and u_1 are the variables at the start of the cycle, i.e., postshock values. When both decay time scales α^{-1} and β^{-1} are small compared to the cycle period Δt, the initial values can be related to the averages over a cycle period as follows:

$$\rho_1 u_1 S_e = \langle \dot{m}_e \rangle (\alpha + \beta) \Delta t, \qquad u_1 = \langle u_e \rangle \beta \Delta t \tag{6}$$

The cycle-average of the dynamic pressure at the exit plane yields the following performance gain:

$$\eta_u = \frac{\alpha + \beta}{\alpha + 2\beta} \beta \Delta t >> 1 \tag{7}$$

Therefore, any unsteady propulsion device with such a strong correlation would produce a higher thrust than a steady engine with similar average values of mass flow and exit velocity. In a steady engine the exit velocity is directly proportional to the sound velocity in the stagnation chamber. In the limit of a large pressure jump at the detonation front, both particle velocity and speed of sound are proportional to the detonation velocity and, therefore, to each other, and to the speed of sound at the end wall of the tube. In that case there is a strong similarity with the steady rocket engine; if the thermal properties of materials impose a limit on the speed of sound in the chamber (as in steady rockets), there is a corresponding limit on the detonation velocity and, therefore, on the exit velocity. Increased performance can then only come from the correlation effect. We emphasize that a high value of the correlation $\langle \rho_e u_e^2 \rangle S_e$ between the mass flow and the velocity at the exit does not create high performance per se, but is rather the characteristic of higher performance. If there is no nozzle present, then the dynamic pressure at the exit plane does not necessarily dominate the static pressure and the $\langle p_e \rangle$ term must also be accounted for.

III. Single-Pulse Optimization

A. Nozzle Shape

We considered five different nozzle shapes (Fig. 1). The tube itself is a cylinder of internal radius $R_i = 2$ cm, and the constant

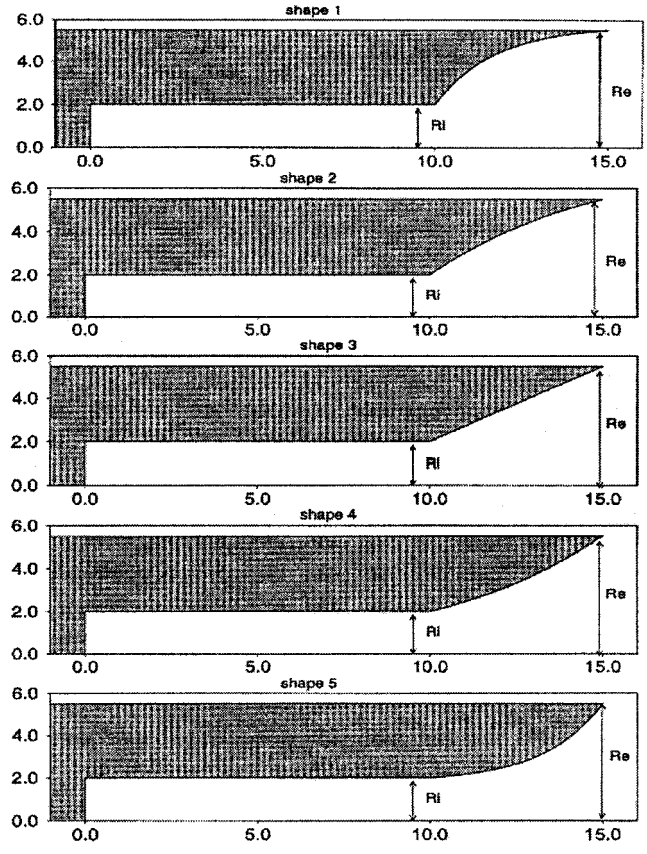

Fig. 1 Schematics of tube and nozzle shapes being studied: Shape 1 ($\eta = -3$), shape 2 ($\eta = -1$), shape 3 ($\eta = 0$), shape 4 ($\eta = 1$), and shape 5 ($\eta = 3$). The reference shape is the straight nozzle, with $R_e = 5.5$ cm and $R_i = 2$ cm.

area section is 10 cm long. The nozzle section is 5 cm long, and the exit radius for the base configuration is $R_e = 5.5$ cm. For one of the nozzle shapes R_e is a parameter of the study. The shapes are described by an exponential law ($y \approx e^{\eta x}$) and, therefore, can be characterized by a unique parameter η. For $\eta < 0$ ($\eta > 0$) the nozzle shape has a negative (positive) curvature, whereas a straight shape is obtained in the limit $\eta \to 0$. The exact formula for the shapes in the nozzle region (from x_i to x_e) is given by

$$y = y_i + (y_e - y_i) \frac{e^{\eta x} - e^{\eta x_i}}{e^{\eta x_e} - e^{\eta x_i}} \tag{8}$$

In the calculations it is generally assumed that the tube and nozzle are initially filled with a stoichiometric hydrogen–air mixture at 1 atm and at a temperature of 350 K, whereas the regions to the right and above the tube are filled with stagnant air at identical conditions (this corresponds to a static test). The tube itself was modeled by a 150 × 20 grid (number of finite volume cells), and the region to the right by an extra 50 cells of gradually increasing spacing. The top section is modeled by a second grid. Quasi-one-dimensional calculations use the same spatial accuracy in the axial direction. This resolution (1-mm spacing) is sufficient for qualitative answers, although the detonation wave profile in the tube is slightly degraded at the front, resulting in a peak pressure that is 85% of the Chapman–Jouguet (CJ) pressure. A more accurate profile can be obtained by increasing the resolution, say, by a factor of 2 or 3, or by using a higher-order scheme than the second-order total variation diminishing (TVD) method used here. Tests with a fourth-order piecewise parabolic method (PPM) show clear improvements, but the computations are significantly more costly (Fig. 2). All computations were performed with the version 2.0 of the MOZART code.[19] Initiation of the detonation is assured by raising the region closest to the left wall

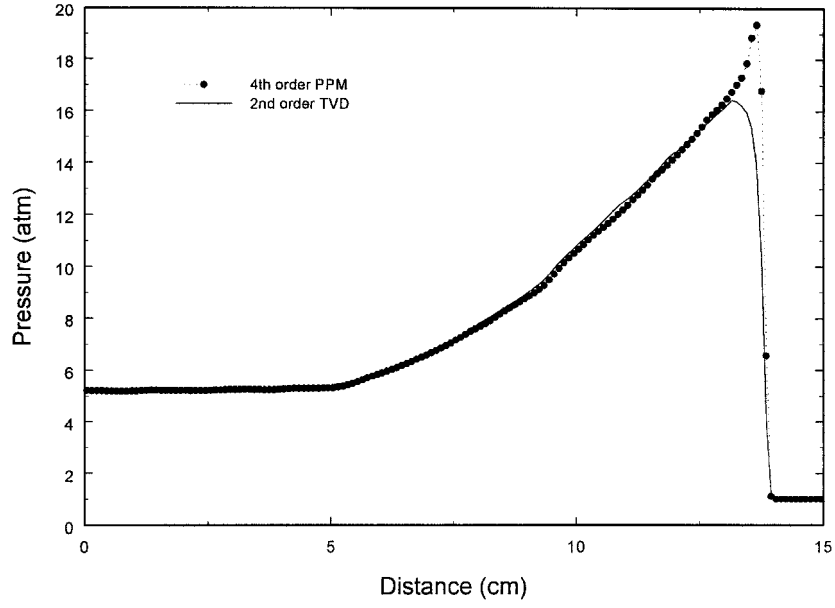

Fig. 2 Detonation wave profiles inside a PDE tube for given resolution. Results from second-order TVD and fourth-order PPM schemes are shown for comparison.

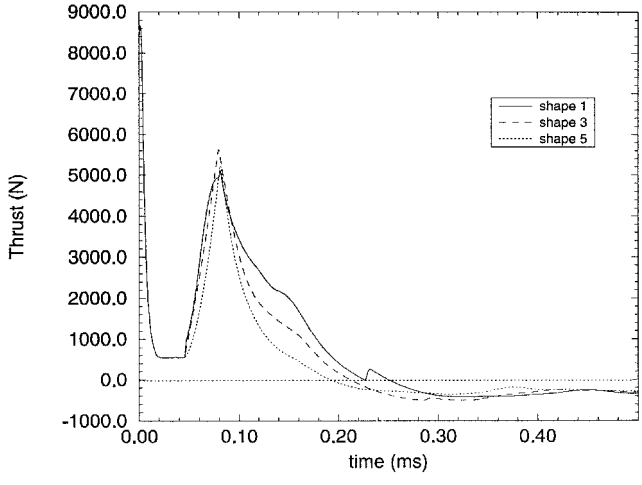

Fig. 3 Instantaneous thrust profiles for shapes 1, 3, and 5 (single pulse).

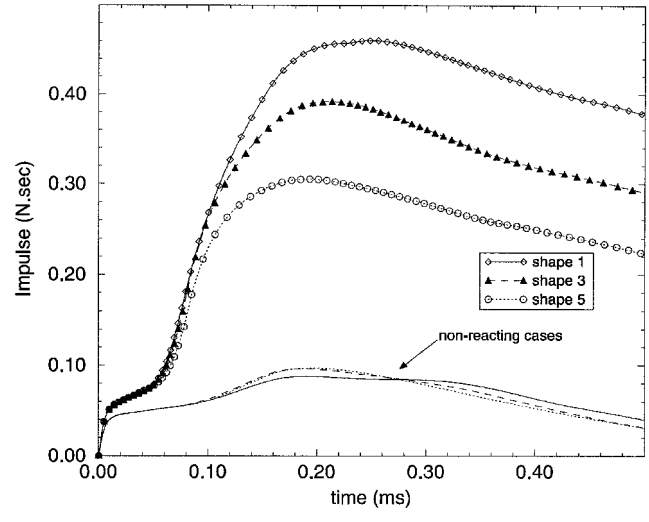

Fig. 4 Integrated impulses as function of time, for shapes 1, 3, and 5. Bottom curves for nonreacting cases indicate the extent of thrust obtained from the energy deposited for the initiation of the detonation.

and of size $\Delta x = 4$ mm to a high pressure (50 atm) and temperature (2500 K). The energy spent in initiating the detonation is therefore the energy spent in compressing the initial, ambient mixture in the tube to these conditions. In the present model the initiation process is a virtual, instantaneous piston operating on a small volume fraction of the tube.

During the calculations, performed for a single pulse in a two-dimensional-axisymmetric configuration, the integrated wall pressure, i.e., the total thrust of the engine, is monitored. The results are shown in Fig. 3 for nozzle shapes 1, 3, and 5. The high peak value at startup is because of the energy deposition near the left wall. This is an artifice of the initiation method, and should not entirely be considered as part of the thrust, unless we have an accurate and realistic model of the ignition. We can estimate the total impulse caused by this ignition mechanism by running a case without chemical reactions and, therefore, without initiating the detonation. This value can then be used to correct the thrust figures. The second, broader peak centered around 0.09 ms corresponds to the detonation wave traveling in the diverging section. The thrust decreases after the detonation wave, with its peak pressure, exits the tube. After 0.20 ms, the thrust takes on negative values, which indicates that the average pressure inside the tube becomes less than the ambient pressure. This is generally the case in the nozzle section. During this part of the blowdown cycle the flow is reversed and the tube is filled with gas from the exhaust region. When the overexpansion is sufficiently large, a shock is formed and moves to the left. A small discontinuity in thrust can be seen for the case of shape 1, at around 0.215 ms, when this weak shock hits the wall at the closed end of the tube.

The total impulse, i.e., force integrated over time, is shown in Fig. 4. Peak impulse is reached when the instantaneous thrust becomes negative. In the same figure, the impulse from the initiation process, estimated by simply computing the flow without chemical reactions, is also shown. The contribution from the initiation process ranges from 17 to 27% of the peak impulse. This obviously affects thrust measurements, and impulse and specific impulse figures should be corrected. One might argue that chemical reactions within the initiation region should also be included, but as mentioned earlier, the actual initiation energy is used only in the pressurization of the critical volume to the required conditions (50 atm, 2500 K).

Ideally, it would be desirable to repeat the cycle immediately after reaching peak impulse. This is not possible because the cycling time depends on the time it takes to refill the tube with fresh mixture. This in turn depends on, among other things, the pressure in the tube. It is therefore necessary to monitor the pressure at the left wall, where the valves are assumed to be located. In Fig. 5, the pressure histories at this location are shown for all five shapes. The backpropagating shock impacts for shapes 1–3 are clearly visible. Because of these shocks it appears that shapes with $\eta > 0$ can lead to slightly higher cycling rates. One of the key factors seems to be the presence/absence of a sharp corner at the nozzle entrance, which induces overexpansion and a backpropagating shock. In an attempt to estimate the impulse for a multicycle process, it is assumed that the refill process can start when the pressure at the left wall reaches a critical value P_c, here set at 1 atm. It must be pointed out from Figs. 4 and 5 that, although the cycling rate is higher for shape 3 compared to shape 1, the impulse at the time of reinjection is larger for shape 1, which seems to indicate that nozzle shapes with negative curvature ($\eta < 0$) are more efficient at thrust production.

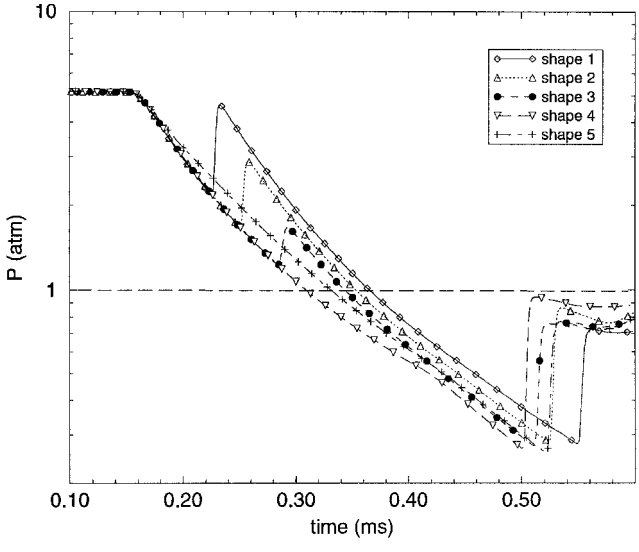

Fig. 5 Time histories of the pressure at the closed end of the tube for all shapes. A first reflected shock is created for shapes with a sharp corner ($\eta \leq 0$). Refueling can occur only after the tube pressure drops below a critical value P_c, set here at 1 atm.

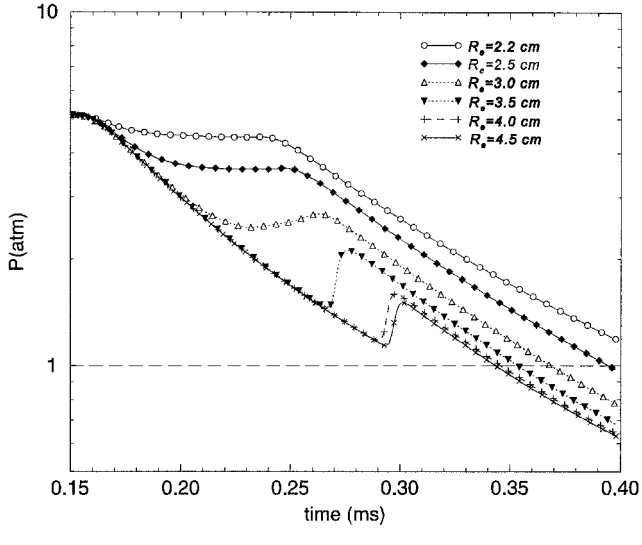

Fig. 6 Time histories of the pressure at the tube closed end, for various cases of exit radius (straight nozzle only).

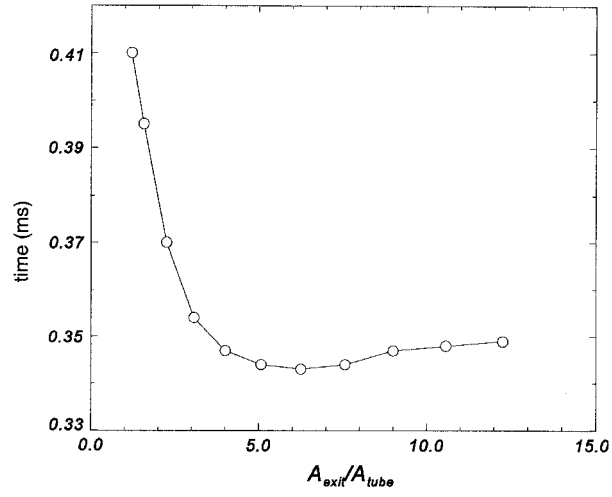

Fig. 7 Time at which refueling can occur, determined by the time at which the pressure at the injection port (closed end) reaches 1 atm, vs the area ratio (straight nozzle).

B. Nozzle Area

In this section the area of the nozzle exit is systematically varied, whereas the tube area is held constant. This is done for shape 3 only and the exit radius is varied from 2.2 to 7 cm, giving a range for the area ratio $A_{\text{exit}}/A_{\text{tube}}$ of 1.21–12.25. The pressure histories at the left wall for different exit radii are shown in Fig. 6 for exit radii up to 4.5 cm. For large values of R_e the profiles are essentially identical, and for clarity they are not shown.

The times at which refueling can proceed (here, when the pressure at the wall reaches 1 atm) as a function of area ratio are shown in Fig. 7. It is clear that the shortest times were obtained for larger area ratios. The use of larger rates of expansion also implies that the net force component in the axial direction (thrust) will be larger. This is demonstrated in Fig. 8a, where the total impulses, measured at peak value and at the time when refueling can occur, are plotted as functions of the area ratio. The corresponding (fuel) specific impulse is shown in Fig. 8b, and for both figures the impulse is corrected by subtracting the contribution of the ignition procedure. The behavior of the specific impulse is quite notable. By increasing the angle of divergence of the nozzle the thrust increases, but so does the volume of the nozzle section (faster than the nozzle area) and the total fuel mass contained in that section. This initially lowers the specific impulse. However, if the effectiveness of the nozzle at delivering thrust increases beyond the simple rule of cross-sectional area increase, the specific impulse may rise again. The exact mechanism for the increase in I_{sp} at higher area ratios is not yet clear.

C. Fuel Distribution

The detonation wave front near the axis of the nozzle may not effectively contribute to thrust on the nozzle walls unless the pressure waves can reach it. Therefore, it is not necessarily advantageous to have fuel distributed over the entire nozzle volume. Instead one may want to keep the fuel close to the walls. This would guarantee a detonation wave near the wall, with its high peak pressure, while minimizing the total amount of fuel being used. To investigate this effect we compute the performance of the tube with only a fuel layer near the wall and compare two strategies for the location and extent of this layer:

1) The constant area section of the tube is completely filled with a fuel–air mixture, whereas the layer of fuel is in the nozzle section only.

2) The fuel layer is in both the constant area section and the nozzle section.

The variation in fuel–air mixture for both of these cases was done by initializing the tube with the mixture in a specified number of computational cells close to the surface of the tube. This is only an approximation to a constant thickness layer because the configuration is mesh dependent. The results for both cases are shown in Fig. 9 as function of the total amount of fuel mass present in the engine at startup. By injecting a layer of fuel in the nozzle section only, we can also achieve a 10% increase in cycling rate (at least based on single-pulse calculations). This is because of the backpropagating shock delay, which increases the pressure on the left wall and increases the time required for it to drop below the fill pressure (Fig. 3). Figure 9 shows the specific impulse (again, corrected for the contribution because of the initiation procedure). The measured total impulse is slowly decreasing as the total amount of fuel present in the tube is being reduced. However, from Fig. 9 we see that it is possible to increase the specific impulse by at least 50%. This corresponds to a thin layer of fuel, and because the calculations do not resolve the induction length, it remains to be seen if a detonation can propagate under these conditions. Typically, one requires a minimum film height of the order of several detonation cell widths, but it is always possible to rescale the engine to guarantee this minimal thickness.

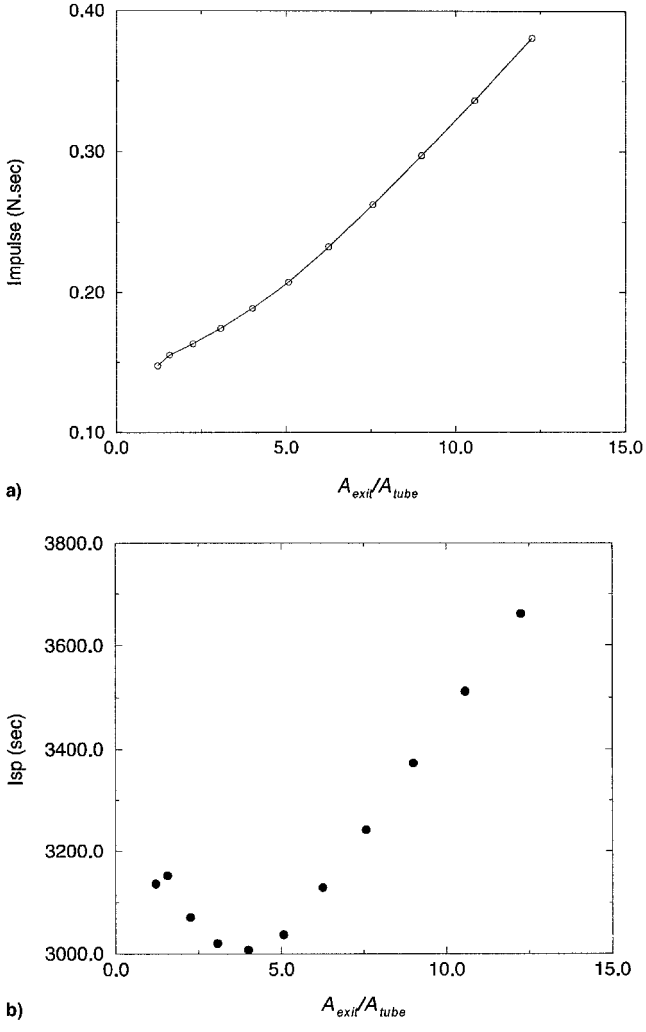

Fig. 8 a) Total and b) specific impulses (single pulse) as functions of area ratio. Impulse measured at refueling time (P_c = 1 atm) and corrected for the ignition energy.

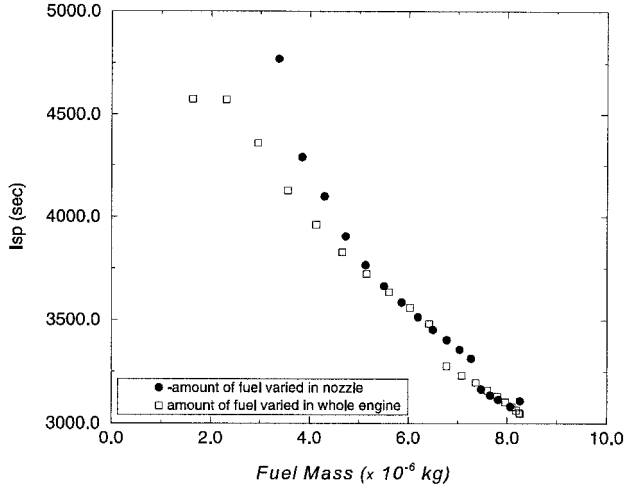

Fig. 9 Specific impulse for the two fuel-layer strategies, as a function of fuel-layer thickness.

IV. Multicycle Optimization

A. Injection Pressure

For this study we use the quasi-one-dimensional version of the code, and consider nozzle shape no. 3 (straight nozzle), with the reference exit radius of 5.5 cm. Refueling occurs when the chamber pressure at the closed end of the tube drops below a critical value P_c. The injection then proceeds using a reservoir pressure P_r, and using the whole surface of the tube cross section for injection. The injection is sonic if the chamber pressure is sufficiently low, i.e., less than the pressure at sonic conditions. If the chamber pressure is too high, injection proceeds through an expansion to lower than sonic conditions,

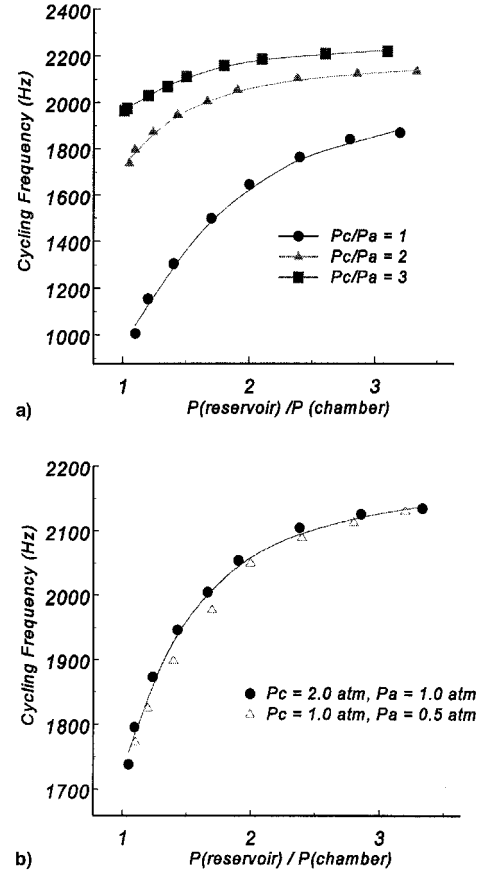

Fig. 10 Cycling frequency obtained from quasi-one-dimensional multicycle computations (straight nozzle, reference nozzle expansion), as function of the ratio of injection pressure over chamber pressure at the time of injection. In Fig. 10b all pressures (P_r, P_c, and P_a) are scaled by the same amount: a) cycling frequency vs pressure ratio and b) universal curve of cycling frequency.

and with less than maximum mass flow. The remaining parameter is the ambient pressure P_a at the exit of the engine. We then measure the cycling frequency that can be attained for these idealized conditions. The results are shown in Fig. 10a for three cases of ratios of critical chamber pressure to ambient pressure P_c/P_a. It would seem a priori that when the reservoir pressure is very close to the chamber pressure at the injector location the mass flow is reduced and the refill delay would be large. This can be verified in Fig. 10a, particularly for the lower curve. However, this also depends on the strength of the rarefaction wave in the tube at the time of injection, which depends on the ratio P_c/P_a. It is clear that when the chamber pressure is much higher than the ambient pressure the peak cycling frequency increases significantly and is less sensitive to the injection pressure. When all three pressure parameters are simultaneously scaled by the same factor, one should recover identical results. This is verified in Fig. 10b, where we compare the cycling frequency for the case $P_c/P_a = 2$, when the ambient pressure is 1 and 0.5 atm. The small difference (less than 1%) is consistent with measurement errors. It could also be partially explained by a small deviation from a linear scaling law, because of chemical recombination. When all three pressure parameters were scaled by the same factor, it was verified that thrust and mass flow scaled proportionally, while the specific impulse remained constant.

For air-breathing configurations at takeoff there is no pressurization available, except by mechanical means. The small pressure ratio required, however, allows the use of low-pressure turbopumps. If this option is not desirable, referring to Fig. 10a shows that even when both pressure ratios are unity the theoretical cycling frequency is still reasonably large.

B. Recharge Timing

The average thrust can be derived in a multicycle computation from the slope of the total impulse delivered to the engine, as a function of time. This impulse in turn can be obtained as the integral over all wall surfaces, i.e., the left-hand side (LHS) of Eq. (4), or from the difference between the exit and inlet conditions, i.e., RHS of Eq. (4). Both are shown in Fig. 11 for the reference case of a straight nozzle with R_e = 5.5 cm. The ambient pressure is atmospheric, the reservoir pressure is 5 atm, and the tube is refilled for P_c = 2 atm. The average thrust is approximately 500 N, and the values from both types of measurement are in excellent agreement. This provides an essential check on the accuracy of our measurements. It must also be pointed out that to achieve this quality of agreement one must be careful to evaluate the impulses at each time step. If the forces were measured with a given sampling rate, e.g., every five iterations, one would observe differences between the two measurements, depending on that sampling rate. For closed-end ignition the integration of wall pressure would give higher accuracy. This is perfectly understandable because at the exit plane one must measure a very narrow profile of total pressure as the detonation crosses the plane. If the sampling rate is low, the peak values may be completely missed. For the same reason, in open-end ignition configurations, the exit plane measurement would be more accurate at low sampling rates. In all subsequent performance results the agreement between the two measurement methods has been checked and is always found to be excellent.

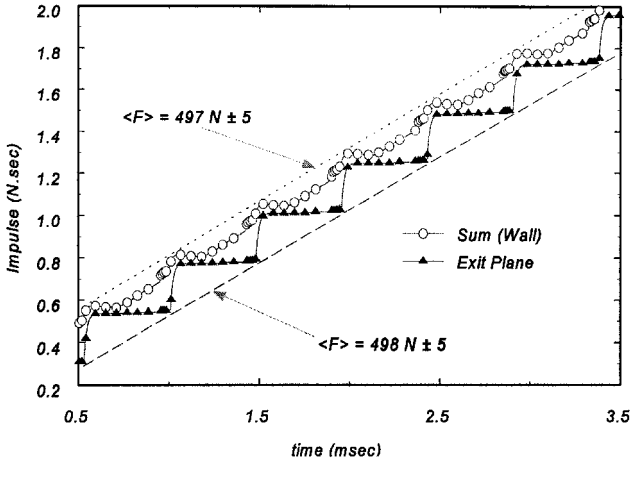

Fig. 11 Multicycle quasi-one-dimensional results, showing the measured total impulse as a function of time. The slopes for the two measurement methods are also indicated and give identical values of the cycle-average force.

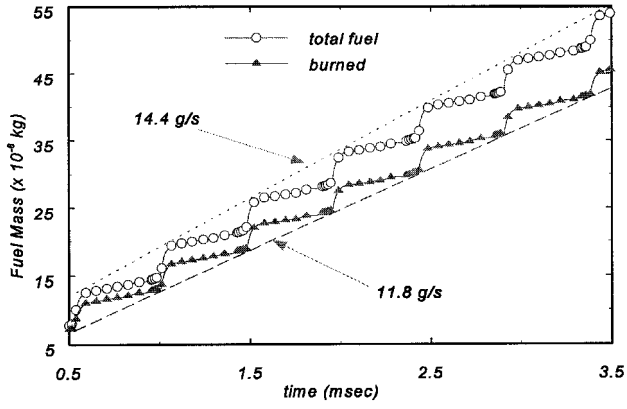

Fig. 12 Total mass of fuel and burned fuel as a function of time. Slopes are indicated and give mass flow rates.

We can also keep track of the fuel injected by monitoring the flow at the exit plane rather than the injection port. This allows us to also monitor the fraction of fuel that is burned, i.e., combustion efficiency. From all species we sum up the fractions made of the hydrogen element. The burned fuel is composed of all species except the unburnt fraction, which is pure H_2. Both masses are plotted as function of time in Fig. 12. The slopes give the fuel mass flows, which are used in turn to determine the average specific impulse. In the present case the fuel I_{sp} is 3540 s. However, the burned fraction is only 82%. This is a surprisingly low efficiency, but it turns out that it is not due to combustion losses, as explained next.

The second parameter that determines the cycling rate is the time at which the injection phase stops and ignition occurs. This is determined in our simulations by the location of the interface between the fresh mixture and the exhaust gases. This is equivalent to setting up a chemical sensor at a specific location to determine the best time to ignite the mixture. Up to this point the results were obtained by selecting a sensor location approximately 1 cm before the exit plane. Conceivably, there may be some fuel leakage past the nozzle exit plane before the detonation reaches that position, and this would lower the efficiency. Therefore, we made a series of calculations where the sensor location (and therefore the time allowed for the injection phase of the engine cycle) is systematically varied. The results are shown in Fig. 13 as a function of the sensor position. We remind the reader that the calculations are for the straight reference nozzle, which starts at 10 cm and the exit plane is at 15 cm.

The fuel losses are dramatically reduced when the fresh charge is allowed to enter only the start of the nozzle before ignition. The cycling frequency also increases, which is expected because the time spent in refueling is lower. However, the rate of increase is lower when the sensor approaches the start of the nozzle. This may be a result of flow characteristics, notably the presence of a shock in the nozzle. Downstream of the shock the velocity decreases and it takes a longer time to fill this section of the nozzle. This may also explain the behavior of the thrust curve, which shows a maximum at some position within the nozzle. The specific impulse consistently

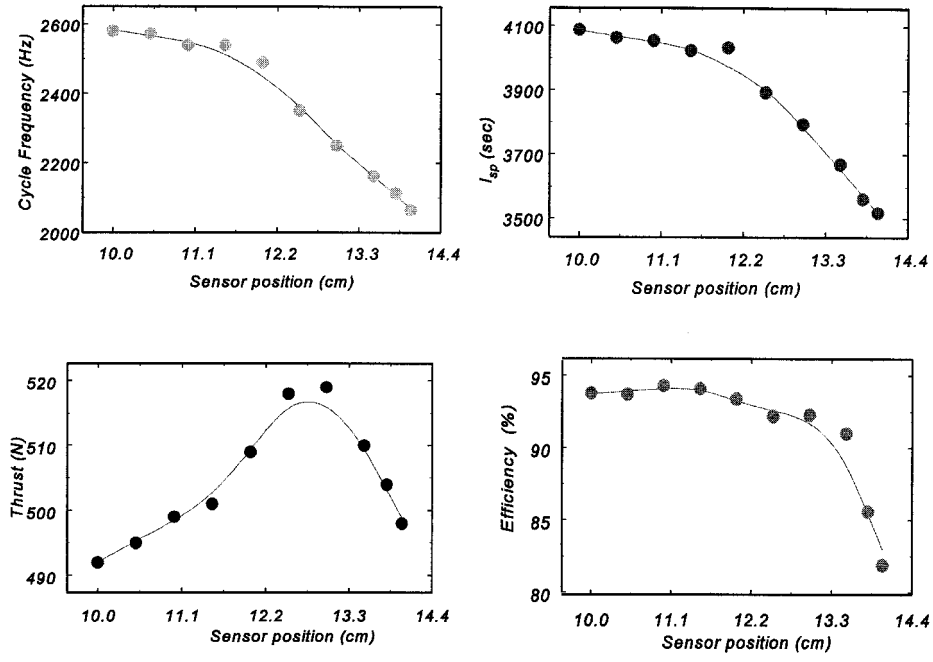

Fig. 13 Variation of performance parameters with respect to second timing parameter, the position of fresh charge sensor. Start of nozzle is at 10 cm, end of nozzle is at 15 cm. Efficiency is ratio of burned fuel to total fuel charge.

increases as the extent of refueling is diminished. However, most of the increase occurs before the sensor moves up to about 12 cm. Ideally, one would therefore want to fill the engine up to the location of the quasisteady shock in the expanding nozzle. Of course, the location of this nozzle shock and, therefore, the optimal timing for ignition, depends on the flow characteristics and will be different for various flight conditions.

C. Open-End Ignition

To conclude the multicycle studies in a quasi-one-dimensional case, we examined one case where the detonation was initiated near the end of the constant area section of the tube. The same energy deposition (50 atm, 2500 K) was used. The performance was then measured and the results were obtained with a sufficiently large number of cycles to achieve good accuracy. The open-end ignition gave us nearly the same amount of average thrust; 489 N compared to 509 N, but the specific impulse was lower at 3500 s, compared with 3975 s for the closed-end ignition. In addition, the cycling frequency was also much lower; 1970 Hz, compared with about 2500 Hz. It would appear for this configuration, i.e., no coupled inlet, that open-end ignition gives a lower performance. We must be careful however not to generalize, because there may be configurations for which open-end ignition gives a higher performance. Nevertheless, this result confirms that obtained in Ref. 9 for a single pulse only.

D. Nozzle Area Revisited

We also performed calculations for several values of the nozzle expansion ratio for the straight nozzle. The specific impulse is plotted as a function of the expansion ratio in Fig. 14. Two cases of reservoir conditions were studied; $P_r = 5$ and 2.2 atm. In both cases, the chamber pressure at injection time was 2 atm, while $P_a = 1$ atm. The injection was stopped when the fresh charge was detected at $x_s = 13.8$ cm. Surprisingly, we see the performance decrease as the area ratio increases. This seems to contradict the earlier results based on single-pulse calculations (Fig. 7). To investigate this result we compared the thrust and impulse histories for two cases of nozzle exit radii (for case $P_r = 2.2$ atm). Both cases are shown in Fig. 15 and indicate that the impulse per cycle is larger for an increased nozzle area, as previously shown in section IIIB. However, the cycle-averaged performance, i.e., the impulse per unit time, is lower when the nozzle area increases because the cycle frequency is lower. The cycling frequency drops with A_e/A_i faster than the thrust per cycle can increase; 1647 Hz for $R_e = 6.5$ cm, and 1978 Hz for $R_e = 4.5$. The corresponding impulses given per cycle can be read from Fig. 15b to be 0.18 and 0.16 N s. This gives us a ratio of average thrust of 94% and, therefore, a decrease in thrust and I_{sp}.

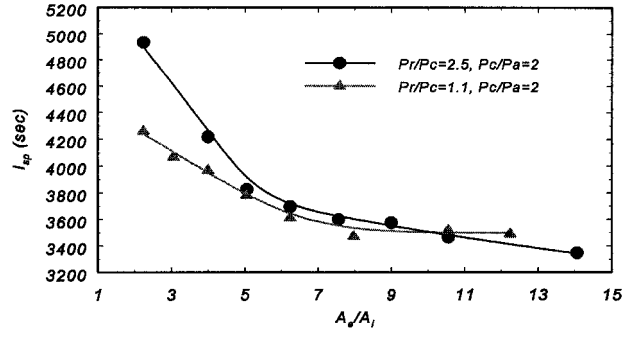

Fig. 14 Specific impulse vs nozzle area ratio for two cases of reservoir pressure. Refueling is stopped when fresh charge is detected 1.2 cm from the exit.

The other change from single-pulse calculations concerns the density profiles within the tube at ignition time. The mixture injection from the closed-end results in a density decrease along the axial distance. Thus, the detonation wave will have a lower peak value at the entrance to the nozzle. This is in marked contrast to the single-pulse calculations, which assumed constant values before ignition.

Constant profiles in the tube can be obtained if one waits long enough for the flow to settle in the tube before injection, and if the injection proceeds in a very specific way. Another method would be to provide another valve at the outlet, which can be used to confine the fresh mixture and pressurize the tube. In both cases one would recover the results from the single pulse study. However, if the objective is to cycle rapidly to provide high average thrust, the fresh charge must be intro-

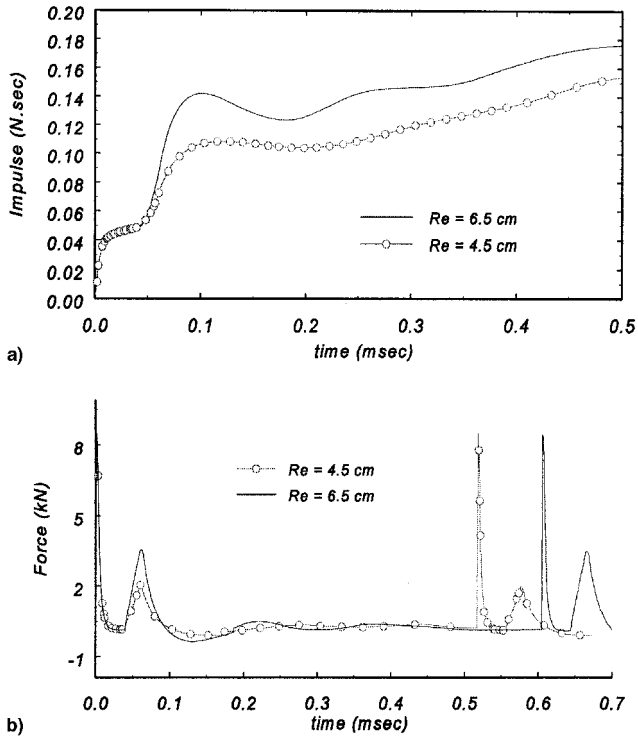

Fig. 15 a) Thrust and b) impulse provided in one cycle, two cases of exit radius, and for P_r/P_c = 1.1. Time and impulse figures reset to start of pulse (ignition) for each case.

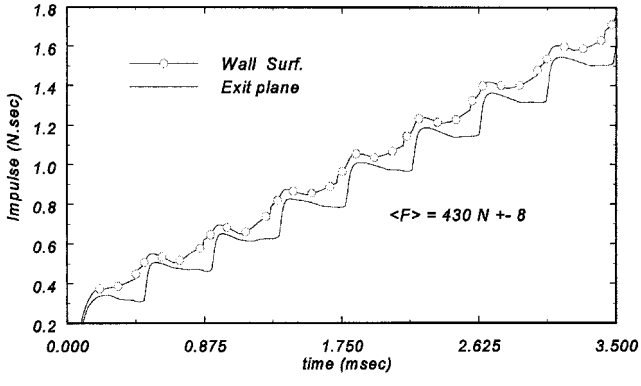

Fig. 16 Impulse trace (wall integration and exit plane) for axisymmetric two-dimensional calculations. Conditions are for straight, reference nozzle, with fresh charge sensor at 14 cm. Corresponding value of average thrust for quasi-one-dimensional calculation was 498 ± 5 N. Notice the impulse drop, as measured at exit plane, during part of blowdown phase.

duced before the flow becomes quiescent, with as high pressure ratios as possible.

E. Two-Dimensional Calculations

We performed some multicycle computations in two-dimensional cases and compared one case with the quasi-one-dimensional computations. The performance results for that case (reference nozzle, sensor at 14 cm) are shown in Fig. 16, and should be compared with the corresponding quasi-one-dimensional results of Fig. 11. Quasi-one-dimensional computations require appropriate boundary conditions on the right side of the nozzle exit plane. Throughout this paper, an infinite reservoir at constant pressure was assumed and a characteristic boundary condition was used. The problem is that the conditions immediately to the right of the nozzle exit are not constant. Examination of the flow dynamics showed that the nozzle shock formation inside the nozzle was much faster in quasi-one-dimensional than in two-dimensional cases, because the two-dimensional calculations correctly reproduced the lowering of the pressure to the right of the exit plane during the blowdown phase. Without this early shock formation the pressure in the nozzle remains low and negative thrust is produced. This is most easily seen by looking at the impulse curve measured at the exit plane, which clearly shows a dip for the two-dimensional case (Fig. 14), while it remains approximately constant in the quasi-one-dimensional case (Fig. 12a).

It was also noticed that it takes more cycles in a two-dimensional case to achieve the true periodic state. This was observed from measuring the slopes of the impulse curve. The slope estimates, i.e., average thrust, were different if only the first three cycles were used, compared to using the last four cycles. In quasi-one-dimensional cases the periodic state is obtained almost immediately. Again, this can be explained in terms of boundary effects.

V. Concluding Remarks

The parametrization of PDE performance is a difficult task, principally because it requires special analytical tools, the number of parameters can be relatively large, and they may be coupled to each other. Therefore, identifying the correct analytical methods, additional scaling laws, and parameter coupling can provide some guidance toward PDE optimization. Although the results presented here are limited in scope, there are a number of important conclusions that we can draw.

1) There can be a significant difference between results based on single-cycle and multicycle computations, and one must exercise caution in their interpretations. There is also a difference between quasi-one-dimensional and multidimensional results, principally because of boundary effects.

2) The common assumptions made for initiation (energy deposition) contribute a nonnegligible fraction of the thrust, and one should eventually devise a method to isolate this contribution during multicycle computations. Similarly, the fuel and oxidizer injection can contribute to the thrust for some conditions ($P_r >> P_c$).

3) Based on single-cycle results, nozzles can increase the thrust delivered during one cycle. The bell-shaped nozzles appear to give a higher performance than shapes with positive curvature. However, nozzles also affect the flow dynamics and, therefore, the timing of the various phases of the engine cycle.

4) There is the potential for a considerable increase in performance by distributing the combustible mixture near the thrust walls only.

5) The cycling rate can be increased by appropriately selecting the pressure at injection time, and with a moderate pressurization of the fuel and oxidizer reservoirs. There is perfect scaling with respect to the three fundamental pressure parameters: 1) reservoir, 2) chamber and 3) ambient pressures.

6) There is a complex dependence of the performance on the flow dynamics, and some indication that the shock position within a nozzle is another performance parameter. It is disadvantageous to attempt to fuel the tube past this shock position.

7) When high cycling rate is desired and, therefore, when the mixture is injected before the flow in the tube completely settles, the nozzle may not provide a performance advantage.

It would appear that very high performance could be achieved by combining some of these results. Constant area tubes offer higher performance at low-flight speeds (high P_a), when high thrust (and high cycling rate) is desirable. However, for high-altitude cruise or space propulsion the situation may be different. The fuel injection may be configured such that the flow conditions before ignition are near constant (similar to the single-pulse assumptions), and the nozzle can play an important role.

One of the most interesting result concerns the effect of a fuel layer near the wall. With this type of fuel distribution, it would also seem very advantageous to inject from the side

walls, i.e., side loading, rather than from the tube front wall (front loading). It may then be possible to obtain another jump in cycling performance, although this remains to be verified by a complete series of multicycle two-dimensional calculations. The fuel-layer configuration is potentially very effective because it essentially is an unsteady ejector. The potential benefits of this particular configuration were first mentioned in Ref. 20, and are derived from the strong coupling with a flowing secondary airstream (the bypass stream). As the detonation wave propagates through the fuel-oxidizer layer, it will generate an oblique (or bow) shock in the bypass air, followed by a contact surface, which acts as a virtual piston. This periodic action will result in the acceleration of slugs of air in the bypass stream, as long as the detonation wave propagates faster than the secondary airstream. Because this unsteady ejector configuration relies on pressure wave rather than viscous coupling, there is less dissipation and higher potential efficiency. It may also be considered for extending the air-breathing PDE flight envelope beyond Mach 3.

The question of nozzle optimization is not completely resolved, and this is an example of the difficulties associated with optimization of this type of engine, when a large number of parameters are coupled. The differences between the single- and multipulse results arise from a logical chain of events: As the blowdown phase affects the flow in the tube at the time of injection, the fresh mixture profiles are affected in turn. The detonation wave and thrust history of the next ignition phase are then dependent on the flow characteristics during the entire cycle and, therefore, on the nozzle shape and expansion ratio, but also on the characteristics of injection, such as pressure and mass flow, injector location, etc. A nozzle with variable geometry would provide a way to optimize the performance throughout the flight regime, but it would also add to the engine complexity and weight. It would also be desirable to minimize the drag created by the low-pressure regions in the nozzle, during the blowdown phase. Ideally, the nozzle area ratio should change within the cycle itself and adapt itself to the local conditions. Clearly, there is no possibility to design a mechanical nozzle capable of adaption on the time scales of the PDE engine cycle. However, we do not discount fluid interactions. This, and the potential performance increase from a pulsed ejector configuration, lead us to believe that the fluid interactions with an ambient or secondary stream should be the main focus of future work.

References

[1]Bussing, T. R. A., and Pappas, G., "Pulse Detonation Engine Theory and Concepts," *Developments in High-Speed Vehicle Propulsion Systems*, Vol. 165, Progress in Astronautics and Aeronautics, AIAA, Reston, VA, 1996.

[2]Azoury, P. H., *Engineering Applications of Unsteady Fluid Flow*, Wiley, New York, 1992.

[3]Cambier, J.-L., and Adelman, H. G., "Preliminary Numerical Simulations of a Pulsed Detonation Wave Engine," AIAA Paper 88-2960, July 1988.

[4]Nicholls, J. A., Wilkinson, H. R., and Morrison, R. B., "Intermittent Detonation as a Thrust-Producing Mechanism," *Jet Propulsion*, Vol. 27, May 1957, pp. 534–541.

[5]Eidelman, S., Grossmann, W., and Lottati, I., "Computational Analysis of Pulsed Detonation Engines and Applications," AIAA Paper 90-0460, Jan. 1990.

[6]Eidelman, S., Grossmann, W., and Lottati, I., "Air-Breathing Pulsed Detonation Engine Concept: A Numerical Study," AIAA Paper 90-2420, July 1990.

[7]Eidelman, S., Lottati, I., and Grossmann, W., "A Parametric Study of Air-Breathing Pulsed Detonation Engine," AIAA Paper 92-0392, Jan. 1992.

[8]Eidelman, S., Yang, X., and Lottati, I., "Pulsed Detonation Engine: Key Issues," AIAA Paper 95-2754, June 1995.

[9]Bussing, T. R. A., and Pappas, G., "An Introduction to Pulse Detonation Engines," AIAA Paper 94-0263, Jan. 1994.

[10]Bussing, T. R. A., Hinkey J. B., and Kaye, L., "Pulse Detonation Engine Preliminary Design Considerations," AIAA Paper 94-3200, June 1994.

[11]Bratkovitch, T. E., and Bussing, T. R. A., "A Pulse Detonation Engine Performance Model," AIAA Paper 95-3155, July 1995.

[12]Lynch, E. D., Edelman, R. B., and Palaniswamy, S., "Computational Fluid Dynamic Analysis of the Pulse Detonation Wave Engine Concept," AIAA Paper 94-0264, Jan. 1994.

[13]Lynch, E. D., and Edelman, R. B., "Analysis of Flow Processes in the Pulse Detonation Wave Engine," AIAA Paper 94-3222, June 1994.

[14]Khoklov, A. M., Oran, E. S., and Wheeler, J. C., "A Theory of Deflagration-to-Detonation Transition in Unconfined Flames," *Combustion and Flame*, Vol. 108, 1997, pp. 503–517.

[15]Pegg, R. J., Couch B. D., and Hunter L. G., "Pulse Detonation Engine Air Induction System Analysis," AIAA Paper 96-2918, July 1996.

[16]Eidelman, S., Grossmann, W., Gunners, N.-E., and Lottati, I., "Progress in Pulsed Detonation Engine Development," AIAA Paper 94-2721, June 1994.

[17]Hinkey, J. B., Bussing, T. R. A., and Kaye, L., "Shock Tube Experiments for the Development of a Hydrogen-Fueled Pulse Detonation Engine," AIAA Paper 95-2578, July 1995.

[18]Aarnio, M. J., Hinkey, J. B., and Bussing, T. R. A., "Multiple Cycle Detonation Experiments During the Development of a Pulse Detonation Engine," AIAA Paper 96-3263, July 1996.

[19]Cambier, J.-L., "Development of Numerical Tools for Pulsed Detonation Engine Studies," The Aeronautical Research Inst. of Sweden, FFA-TN 1996-50, Bromma, Sweden, Oct. 1996.

[20]Cambier, J.-L., Adelman, H. G., and Menees, G. P., "Numerical Simulations of a Pulsed Detonation Augmentation Device," AIAA Paper 93-1985, June 1993.